Analysis of Phasor Measurement Method in Tracking the Power Frequency of Distorted Signals

Ramin Agha Zadeh, Arindam Ghosh, Gerard Ledwich and Firuz Zare

Queensland University of Technology
GPO Box 2434, Brisbane,
QLD, 4001, Australia
ramin.aghazadeh@qut.edu.au

Abstract

This paper presents an analysis of phasor measurement method for tracking the fundamental power frequency to show if it has the performance necessary to cope with the requirements of power system protection and control. In this regard, several computer simulations presenting the conditions of a typical power system signal especially those highly distorted by harmonics, noise and offset, are provided to evaluate the response of the Phasor Measurement (PM) technique. A new method, which can shorten the delay of estimation, has also been proposed for the PM method to work for signals free of even-order harmonics**.**

1. Introduction

Control and protection of power system include real time estimates of system frequency. The faster and more precise are the estimates, the more reliable are the related control and protection schemes. Harmonic and noise contamination have become a major concern for power system since this affects the accuracy of the estimates and the speed of estimation. Besides, the integration of power electronic devices to utility grids necessitates a reliable estimator not only to provide service to linear loads but also to compensate/cater for nonlinear loads. Various techniques have been introduced in the literature to estimate the power frequency. One of the most common techniques to estimate the frequency of signal is the zero crossing detection method and its modifications [1-3]. Multiple zero crossing and inaccuracies due to noise and harmonic distortions are the major issues that these methods should take care of. Zero-crossing methods do not respond quickly to the frequency changes in a distorted signal [4] and their performance is sensitive to the type of signal transients [1,5]. Linear estimation of phase (LEP) [6,7], Decomposition of Single Phase into Orthogonal Components (DSPOC) [8,9], Discrete Fourier Transform (DFT) with Phase Compensation [1] and the modifications of this method [1], [10,11] perform extremely well but they all suffer from a periodic error in the estimated frequency if it departs from the assumed frequency. This can be cancelled using a low pass filter although it would introduce delays and obscure any real oscillations in the fundamental frequency [12].

Kalman filtering [13-15], phase locked loop (PLL) [4], least square (LS) [16,17], Newton type algorithms [18], and adaptive notch filters [19] are among the other existing techniques for frequency estimation. References [2], [12] and

[20,21] review these techniques. These methods have their strengths and drawbacks. This paper conducts an in-depth analysis on the PM technique which reveals its strengths and drawbacks. The analysis will be followed by a new technique proposed to enhance the speed of the PM technique while the input signal is free of even-order harmonics.

The rest of the paper is organized as follows. In Section 2, algorithms required for the phasor measurement method are derived. The analysis of this technique calls for setting some crucial parameters and models in the simulation tests. These issues and recommended solutions are explained in Section 3. Performance of this method is evaluated for different simulated conditions. Its immunity to noise and distortion as well as its tracking speed in response to any changes in the signal attributes are highlighted in Section 4. Section 5 summarizes the main conclusions of the paper.

2. Development of PM algorithms

2.1. Basic PM-Technique

A typical power system or power electronic signal can be expressed as follows.

$$v(t) = a_1 \sin(2\pi f t + \theta_1) + h(t) + n(t) + v_{off}(t) \tag{1}$$

where a_1 , θ_1 and f denote the amplitude, initial phase angle and frequency of the fundamental component, respectively. Symbols $h(t)$, $n(t)$ and $v_{off}(t)$ represent the harmonic, noise and offset parts of the signal, respectively. Signal offset is often produced in the measurement and data conversion process using A/D devices. Harmonics, noise and offset always cause errors in the estimation of the frequency. However, the theoretical model of the signal is assumed to be noise free and then can be expressed as

$$v(t) = a_1 \sin(\omega t + \theta_1) + \sum_{k=2}^{+\infty} a_k \sin(k\omega t + \theta_k) + v_{off}(t) \tag{2}$$

where a_k denotes the amplitude of the k^{th} harmonic component and θ_k denotes the initial phase angle of the harmonic component when the phase angle of the fundamental component is zero. Initial phase angles of harmonics are usually produced as a result of different phase shifts imposed by low pass filters installed at output points of power electronic converters.

A typical three phase signal can also be expressed by three different equations in the form of (2). The transformation of this three phase signal in to the *dq* form gives its rotational *dq*-phasor. From (2) and for unbalanced three phase signals, the relevant phasor can be produced in the following form.

$$Y(t) = K_0 + r_1^{+} e^{j(\omega t + \theta_1^{+})} + r_1^{-} e^{-j(\omega t - \theta_1^{-})} + \sum_{i=2}^{+\infty} r_i^{+} e^{j(i\omega t + \theta_i^{+})} + \sum_{i=2}^{+\infty} r_i^{-} e^{-j(i\omega t - \theta_i^{-})} \tag{3}$$

where K_0 is the dc term of the signal phasor and symbols r_1^{+} and r_1^{-} represent respectively the positive and negative sequence amplitude of the i^{th} harmonic. Also, θ_i^{+} and θ_i^{-} represent respectively the positive and negative sequence initial phase angle of the i^{th} harmonic.

The following integration is used in the phasor measurement technique of this paper. The integration is another presentation of discrete Fourier transformation proposed in [10].

$$S(t,\tau) = \int_{t}^{t+\tau} Y(t')e^{-j\omega_0 t'}dt' \tag{4}$$

where $\omega_0=2\pi\times50$ rad/sec, $t+\tau$ indicates the online instant of estimation and τ denotes the integration period.

From (3) and (4) let us define the following equations.

$$S_0(t,\tau) = \int_{t}^{t+\tau} K_0 e^{-j\omega_0 t'}dt' = K_0 \frac{e^{-j\omega_0\tau}-1}{\omega_0} e^{j\left(\frac{\pi}{2}-\omega_0 t\right)} \tag{5}$$

$$S_i^+(t,\tau) = \int_{t}^{t+\tau} r_i^+ e^{j\left(i\omega t'+\theta_i^+\right)} e^{-j\omega_0 t'}dt' = \frac{r_i^+}{\Delta\omega_i} e^{j\left(\Delta\omega_i t+\theta_i^+-\frac{\pi}{2}\right)}\left(e^{j\Delta\omega_i\tau}-1\right) \tag{6}$$

where $\Delta\omega_i=i\omega-\omega_0$

Using the formula:

$$e^{j\alpha}-1 = 2\sin\left(\frac{\alpha}{2}\right)e^{j\left(\frac{\alpha}{2}+\frac{\pi}{2}\right)} \tag{7}$$

(6) can be rewritten as:

$$S_i^+(t,\tau) = \frac{2r_i^+}{\Delta\omega_i}\sin\left(\frac{\Delta\omega_i\tau}{2}\right)e^{j\left(\Delta\omega_i t+\theta_i^+\right)}e^{\frac{j\Delta\omega_i\tau}{2}} \tag{8}$$

Again from (3) and (4), the following integration for the negative sequence components can be obtained.

$$S_i^-(t,\tau) = \int_{t}^{t+\tau} r_i^- e^{-j\left(i\omega t'-\theta_i^-\right)} e^{-j\omega_0 t'}dt' = \frac{r_i^-}{\hat{\omega}_i} e^{-j\left(\hat{\omega}_i t-\theta_i^--\frac{\pi}{2}\right)}\left(e^{-j\hat{\omega}_i\tau}-1\right) \tag{9}$$

where $\hat{\omega}_i = i\omega+\omega_0$

From (5) to (9) the magnitudes of the integrations can be obtained as

$$\left|S_0(t,\tau)\right| = K_0\frac{\left|e^{-j\omega_0\tau}-1\right|}{\omega_0} \tag{10}$$

$$\left|S_1^+(t,\tau)\right| = \left|\frac{r_1^+}{\Delta\omega_1}\left(e^{j\Delta\omega_1\tau}-1\right)\right| = \left|\frac{2r_1^+}{\Delta\omega_1}\sin\left(\frac{\Delta\omega_1\tau}{2}\right)\right| \tag{11}$$

$$\left|S_i^+(t,\tau)\right| = \frac{r_i^+}{\Delta\omega_i}\left|e^{j\Delta\omega_i\tau}-1\right| = \frac{2r_i^+}{(i-1)\omega_0+i\Delta\omega_1}\left|\sin\left(\frac{\Delta\omega_i\tau}{2}\right)\right| \tag{12}$$

Since $\Delta\omega_1\tau$ is small, (11) can be approximated as

$$\left|S_1^+(t,\tau)\right| \approx \left|\frac{2r_1^+}{\Delta\omega_1}\left(\frac{\Delta\omega_1\tau}{2}\right)\right| = r_1^+\tau \tag{13}$$

However, the same approximation is not applicable for $|S_i^+(t,\tau)|$ in (12) while $i > 1$ because $\Delta\omega_i$ is not small. For $i > 1$ the following inequality can be deduced from (12)

$$\left|S_i^+(t,\tau)\right| \le \frac{2r_i^+}{(i-1)\omega_0+i\Delta\omega_1} \le \frac{2r_i^+}{\omega_0-2\left|\Delta\omega_1\right|} \tag{14}$$

From (9) the followings can be obtained.

$$\left|S_i^-(t,\tau)\right| = \frac{r_i^-}{\hat{\omega}_i}\left|e^{-j\hat{\omega}_i\tau} - 1\right| \le \frac{2r_i^-}{2\omega_0 - \left|\Delta\omega_1\right|} \tag{15}$$

$$\left|S_0(t,\tau)\right| = K_0\frac{\left|e^{-j\omega_0\tau} - 1\right|}{\omega_0} \le \frac{2K_0}{\omega_0} \tag{16}$$

From (13) to (16) it can be deduced that comparing with $|S_1^+(t,\tau)|$, the others, $|S_i^+(t,\tau)|$ and $|S_i^-(t,\tau)|$ as well as $|S_0(t,\tau)|$, are small enough to let simplify the phasor integration by the following approximation. The simulation results provided in Section 4 will present satisfactory levels of accuracy for this approximation.

$$S(t,\tau) \approx S_1^+(t,\tau) \tag{17}$$

From (8) and (17) the following equation can be obtained.

$$\angle S(t,\tau_1) - \angle S(t,\tau_2) = \angle S_1^+(t,\tau_1) - \angle S_1^+(t,\tau_2) = \frac{\Delta\omega_1}{2}(\tau_1 - \tau_2) \tag{18}$$

The integration of the signal in (4) can be directly computed using the samples of the signal. The three phase samples after the *dq*-transformation are manipulated to constitute the signal phasor. The integration of the signal phasor over a period of τ at any instant of t can be obtained using the summation of small trapezoidal parts over the time axis in the graph of the signal. Thus, the integration can be expressed as

$$S(t,\tau) = \left\{\frac{Y(t)e^{-j\omega_0 t} + Y(t+\tau)e^{-j\omega_0(t+\tau)}}{2} + \sum_{i=1}^{n-1}\left[Y(t+i\Delta T)e^{-j\omega_0(t+i\Delta T)}\right]\right\}\tau \tag{19}$$

where n is given by:

$$n = \left\lfloor \frac{\tau}{\Delta T} \right\rfloor \tag{20}$$

From (18) and (19), the online algorithm for the calculation of frequency deviation can be adopted. However, the results of frequency calculations depend significantly upon the selection of τ_1 and τ_2. Let us consider the assumption made in (17) to clarify this dependency.

$$S(t,\tau) \approx S_1^+(t,\tau) \;\Rightarrow\; S(t,\tau) = S_1^+(t,\tau) + e(t,\tau) \tag{21}$$

where *e(t,τ)* represents the error of the approximation. From (3) to (12) and (21) this error can be expressed as

$$e(t,\tau) = S_0(t,\tau) + \sum_{i=2}^{+\infty} S_i^+(t,\tau) + \sum_{i=1}^{+\infty} S_i^-(t,\tau) \tag{22}$$

The components of the error function, defined in (22), usually cause some oscillations in the frequency estimation that can lead to large estimation errors. However, this can be overcome by choosing appropriate values for the integration period. In this regard, the error function can be rewritten in the following manner using (5), (6), (9) and (22).

$$e(t,\tau) = s_0(t,\tau)\left|e^{-j\omega_0\tau} - 1\right| + \sum_{i=2}^{+\infty}\left\{s_i^+(t,\tau)\left|e^{j[(i-1)\omega_0 + i\Delta\omega_1]\tau} - 1\right|\right\} + \sum_{i=1}^{+\infty}\left\{s_i^-(t,\tau)\left|e^{-j[(i+1)\omega_0 + i\Delta\omega_1]\tau} - 1\right|\right\} \tag{23}$$

It is now clear that by choosing $\tau = mT_0$, where m is an integer coefficient and T_0 is the nominal period of signal or *20ms*, the magnitudes of exponential parts, shown in (23), can approach to one. This can decrease the amount of error

components and make the error approach to zero.

$$\tau = mT_0 \Rightarrow e(t,\tau) = s_0(t,\tau)\left|e^{-j\frac{2\pi}{T_0}mT_0} - 1\right| + \sum_{i=2}^{+\infty}\left\{s_i^+(t,\tau)\left|e^{j\left[(i-1)\frac{2\pi}{T_0}+i\Delta\omega_1\right]mT_0} - 1\right|\right\} + \sum_{i=1}^{+\infty}\left\{s_i^-(t,\tau)\left|e^{-j\left[(i+1)\frac{2\pi}{T_0}+i\Delta\omega_1\right]mT_0} - 1\right|\right\} \quad (24)$$

$$\Rightarrow e(t,\tau) = s_0(t,\tau)|1-1| + \sum_{i=2}^{+\infty}\left\{s_i^+(t,\tau)\left|e^{j(i\Delta\omega_1)mT_0} - 1\right|\right\} + \sum_{i=1}^{+\infty}\left\{s_i^-(t,\tau)\left|e^{-j(i\Delta\omega_1)mT_0} - 1\right|\right\} \quad (25)$$

$$\Rightarrow e(t,\tau) = \sum_{i=2}^{+\infty}\left\{s_i^+(t,\tau)\left|e^{j(i\Delta\omega_1)mT_0} - 1\right|\right\} + \sum_{i=1}^{+\infty}\left\{s_i^-(t,\tau)\left|e^{-j(i\Delta\omega_1)mT_0} - 1\right|\right\} \quad (26)$$

Accordingly, the error imposed by the DC offset is totally removed and the errors by other components can be minimized. Therefore, the integration periods of τ_1 and τ_2 in (18) must be chosen as integer coefficients of the main period of the signal. The minimum value arrangement for them is as $1\times T_0$ and $2\times T_0$. Hence, the minimum-size of the data window that can provide accurate estimates of frequency is the integer floor of $2T_0/\triangle T$. Thereby, the formula for the frequency estimation purpose, so-called basic or ordinary PM-technique in this paper, is as follows.

$$\angle S(t,2T_0) - \angle S(t,T_0) = \frac{\omega - \omega_0}{2}T_0 \quad (27)$$

It is obvious that the delay of $2T_0$ must be expected for the estimation results obtained by (27). However, power system signal is usually free of even harmonics where using the technique explained in the following subsection can help use a smaller data window to estimate the power frequency.

2.2. Enhanced PM-Technique

This subsection proposes a new approach for the PM method to work for signals free of even-order harmonics that can shorten the delay of frequency estimation**.** Let us assume that the three phase signals of $v_a(t)$, $v_b(t)$ and $v_c(t)$ are free of even-order harmonics and their dc offsets are the same. The time-domain positive sequence of the signal can be defined as

$$\begin{bmatrix} v_a^+(t) \\ v_b^+(t) \\ v_c^+(t) \end{bmatrix} = \frac{1}{3}\begin{bmatrix} 1 & \beta & \beta^2 \\ \beta^2 & 1 & \beta \\ \beta & \beta^2 & 1 \end{bmatrix}\begin{bmatrix} v_a(t) \\ v_b(t) \\ v_c(t) \end{bmatrix} \quad (28)$$

where $\beta = e^{j2\pi/3}$

Assuming K_a^+, K_a , K_b and K_c as the DC component of $v_a^+(t)$, $v_a(t)$, $v_b(t)$ and $v_c(t)$ respectively, it can be proven that the positive sequence signal is free of DC offset if the DC offset in time-domain is the same for the three phases. From (28) and (3) it can be deduced that

$$3K_a^+ = K_a + \beta K_b + \beta^2 K_c = K_a + (\cos 120^o + j\sin 120^o)K_b + (\cos 120^o - j\sin 120^0)K_c = K_a - \frac{K_b + K_c}{2} + j\frac{\sqrt{3}}{2}(K_b - K_c) \quad (29)$$

Therefore if $K_a = K_b = K_c$ then $K_a^+ = K_b^+ = K_c^+ = 0$. As a result, the phasor of such a signal after the dq-transformation of

its positive sequence components can be expressed as

$$Y(t) = r_1^+ e^{j(\omega t+\theta_1^+)} + \sum_{i=1}^{+\infty} r_{2i+1}^+ e^{j\left[(2i+1)\omega t+\theta_{2i+1}^+\right]} + \sum_{i=1}^{+\infty} r_{2i-1}^- e^{-j\left[(2i-1)\omega t-\theta_{2i-1}^-\right]} \tag{30}$$

The integration period can be chosen to be $T_0/2$ as it is now possible to make the error components to approach zero.

$$\begin{aligned} e(t,\frac{T_0}{2}) &= \sum_{i=1}^{+\infty}\left\{ s_{2i+1}^+\left(t,\frac{T_0}{2}\right)\left| e^{j\left[(2i)\frac{2\pi}{T_0}+(2i+1)\Delta\omega_1\right]\frac{T_0}{2}} - 1\right|\right\} + \sum_{i=1}^{+\infty}\left\{ s_{2i-1}^-\left(t,\frac{T_0}{2}\right)\left| e^{-j\left[(2i-2)\frac{2\pi}{T_0}+(2i-1)\Delta\omega_1\right]\frac{T_0}{2}} - 1\right|\right\} \\ \Rightarrow\ e(t,\frac{T_0}{2}) &= \sum_{i=1}^{+\infty}\left\{ s_{2i+1}^+\left(t,\frac{T_0}{2}\right)\left| e^{j(i+0.5)T_0\Delta\omega_1} - 1\right|\right\} + \sum_{i=1}^{+\infty}\left\{ s_{2i-1}^-\left(t,\frac{T_0}{2}\right)\left| e^{-j(i-0.5)T_0\Delta\omega_1} - 1\right|\right\} \end{aligned} \tag{31}$$

Either for reasonably small values of *i,* $T_0\triangle\omega_1$ is small enough to have the exponential terms of (31) approach one or for large values of *i* the amplitudes of the integration functions, s_{2i+1}^+ and s_{2i-1}^-, are very tiny because of the negligible contribution of very high order harmonics in ordinary power system signals. Therefore, the error function of $e(t,T_0/2)$ will approach zero which is desirable. Hence, a reliable formula can now be built for the frequency estimation purposes which is

$$\angle S(t,T_0) - \angle S(t,\frac{T_0}{2}) = \frac{\omega - \omega_0}{4} T_0 \tag{32}$$

In practice, there is no guarantee that the offset signals of K_a, K_b and K_c always equal to each other. This can lead to the appearance of instantaneously non-zero dc terms in the positive sequence components of K_a^+, K_b^+ and K_c^+. Thus, these DC terms can cause error in the results of estimation by (32). However, using the positive sequence components of the signal, the produced error is less than that when the phasor of the signal is directly obtained from the three-phase signal itself.

3. Discussion on the noise model, high frequency sampling, and random variations of load

There are a number of parameters that should be considered in the development of frequency estimation algorithms using digital sampling of signal. In this section, what these parameters are for the phasor measurement technique of this paper and how they should be modeled, are discussed.

A random noise with zero mean and Gaussian distribution with 0.02*pu* of standard deviation is the typical model of noise used in the simulations of this paper. This signal conventionally models the noise related to the measurement and signal conversion in A/D. Furthermore, an unconventional noise which relates to the high frequency sampling rate of A/Ds is also applied. In spite of reliable clocks and accurate counters used by microprocessor to define the exact instant of performing the sampling subroutines, in practice a variable, slight time delay due to internal loading of microprocessors and internal hardwired interfaces exists for an A/D to receive the sampling command. Also, a variable delay depending upon the A/D's quality and its speed in high frequency ranges must be supposed for the A/D to take the samples right after receiving the command. Therefore, the sampling interval in the simulations has been supposed to be a random signal with Gaussian distribution that has a mean of 40-kHz and 2% standard deviation.

Moreover, the load variation, which can affect the amplitude of current signal and even the amplitude of voltage signal in case of a weak source, can be modelled as a kind of random noise. In particular cases, such as when DG sources integrated to a power grid, the load profile changes instantaneously as the costumers switch their loads on/off randomly anytime. This issue causes slight variations in both the amplitude of current signal as the load impedance changes and the amplitude of voltage signal if the source is not stiff enough to maintain the voltage profile or if a droop control method has been chosen for the application. The droop method [22] can control the voltage changes based on the variations in the real and/or reactive power. Therefore, another random signal of Gaussian distribution with zero mean and 0.02pu of standard deviation has been set as the variant part of the signal amplitude in the simulations.

4. Simulation studies

In this section, the phasor measurement algorithm is evaluated through simulation.

4.1. Frequency tracking

The following test signal is applied to examine the ability of the PM technique in frequency estimation.

$$Y(t) = 0.04 + \left[1 + n_1^+(t)\right]e^{j(\omega t - 10^o)} + \left[0.45 + n_1^-(t)\right]e^{-j(\omega t + 20^o)} + \sum_{i=2}^{15}\left[r_i^+ + n_i^+(t)\right]e^{j(i\omega t + \theta_i^+)} + \sum_{i=2}^{15}\left[r_i^- + n_i^-(t)\right]e^{-j(i\omega t - \theta_i^-)} + n(t) \quad (33)$$

where r_i^+, r_i^- and θ_i^+ as well as θ_i^- are chosen from Table. 1.

Table 1. Characteristics of the test signal

h	r_i^+	θ_i^+	r_i^-	θ_i^-
1	1	-10°	.45	20^0
2	0.06	-18^0	0.05	-30^0
3	0.07	30^0	0.04	45^0
4	0.05	18^0	0.02	-50^0
5	0.05	36^0	0.02	10^0
6	0.03	-30^0	0.03	-36^0
7	0.04	45^0	0.04	9^0
8	0.04	45^0	0.01	-18^0
9	0.03	18^0	0.03	20^0
10	0.02	10^0	0.02	60^0
11	0.03	9^0	0.01	-36^0
12	0.01	-60^0	0.03	-9^0
13	0.04	10^0	0.04	45^0
14	0.03	-20^0	0.02	-18^0
15	0.02	9^0	0.01	50^0

The angular frequency ω in (33) is 100π rad/sec. $n_i^+(t)$ and $n_i^-(t)$ for i=1,2,…,15 denote random noise signals with Gaussian distribution of zero mean and a standard deviation equal to 2 percent of r_i^+ and r_i^-, respectively. These noises are intended to simulate the random changes in the customer load. The offset is 0.04pu and $n(t)$ is a Gaussian random

noise with zero mean and 0.02 *pu* standard deviation. Furthermore, the sampling interval is supposed to be a random signal with Gaussian distribution with a mean which is specified individually at any particular simulation and a standard deviation equal to 2 percent of the specified mean value.

Fig. 1(*a*) shows the result of frequency estimation by the basic phasor measurement technique based on (27). The algorithm can track the frequency successfully in this case. The error is less than 0.012 Hz despite the large noise, offset, unbalance and harmonic distortion being applied. PLL-based techniques, in contrast, suffer from periodical errors. The errors caused by the phase unbalancing, harmonics, and offset in the PLL system have the frequency components of $2\omega_0$, multiples of $6\omega_0$, and ω_0 respectively. To reduce these errors a loop filter with an extremely low bandwidth is required which degrades the dynamic performance [21].

Fig. 1(*b*) shows the frequency estimation result by the basic PM that uses (18) when τ_1 and τ_2 are chosen as T_0 and $T_0/2$ respectively. Periodic errors up to 1Hz can be observed. The comparison of these two figures supports the idea of choosing the integration periods of like mT_0 in (24) to (26) to preclude the oscillatory errors when even harmonics and dc offset are present in the components of signal. Therefore, it can be concluded that for a signal such as that of (33), the minimum data window size of $2T_0$ must be applied. However, this can cause a delay of $2T_0$ in tracking the new targets of frequency.

Fig. 2 shows the result of frequency estimation by the basic PM and (27) for the test signal of (33) when the frequency of the signal suddenly changes from 50Hz to 50.3Hz at t=0.5s. The precision of the estimation results for the off-nominal frequency is also good as the error is low. Some frequency estimation techniques such as Discrete Fourier Transform, Decomposition of Single Phase into Orthogonal Components, and Linear Estimation of Phase already suffer from a periodic error in the estimated frequency if it departs from the assumed frequency even if the input signal is not polluted by noise and harmonic distortions [12]. Moreover, the results of performed simulations show that the response of the basic PM for the frequency drift is exactly the same for the frequency rise.

The frequency estimation shown in Fig. 1(a) is based on the sampling frequency of 40kHz. Fig. 3 shows the result of estimation for the same test signal and the same PM technique but based on 5kHz sampling rate. In this case, the error of estimation can reach up to 0.067Hz. While the response of the proposed method in rather high sampling rates is significant, it is expected to be degraded for low sampling rates. As a matter of fact, this is an inherent property of the approach based on the sample integration. The statistical analysis on the frequency estimation outputs that result by performing the basic PM method of (27) for a range of different sampling frequency rates is highlighted in Table 2. The input signal is like that in (33) except the harmonic components higher than the tenth order are not included. It should be noted that in practice an anti-aliasing filter with cut-off frequency equal to the half of sampling frequency is always used, and that affects the input signal before sampling. (Therefore, the order of harmonic components used in this study will not exceed 10). That is, a common signal can be used for different test cases where its components are always

within the band-pass of the anti-aliasing filters even in the worst case where the cut-off frequency is 500Hz for the sampling frequency of 1 kHz.

Table 2. Result of statistical analysis on frequency estimates

Case No.	Sampling Frequency	Data Average(Hz)	Variance (Hz^2)	Maximum Error (Hz)
1	40kHz	50	2.48×10^{-5}	0.0117
2	20kHz	50	6.75×10^{-5}	0.023
3	10kHz	49.9999	0.98×10^{-4}	0.029
4	5kHz	49.9984	4.15×10^{-4}	0.066
5	1kHz	49.9993	1.39×10^{-3}	0.108

Fig. 4 shows the result of frequency estimation using positive sequence components of a test signal that is the same as that of (33) but free of even-order harmonics. The test signal in this case is as follows.

$$Y(t) = \left[1 + n_1^+(t)\right]e^{j\left(\omega t - 10^o\right)} + \left[0.45 + n_1^-(t)\right]e^{-j\left(\omega t + 20^o\right)} + \sum_{i=1}^{7}\left[r_{2i+1}^+ + n_{2i+1}^+(t)\right]e^{j\left[(2i+1)\omega t + \theta_{2i+1}^+\right]} + \sum_{i=1}^{7}\left[r_{2i+1}^- + n_{2i+1}^-(t)\right]e^{-j\left[(2i+1)\omega t - \theta_{2i+1}^-\right]} + n(t) \tag{34}$$

It should be noted that the original three-phase-signals have been set to have 0.04 pu offset signal but the phasor, Y(t), in (34) becomes free of any dc terms after applying the process described in (28) and (29). Therefore, the enhanced PM method based on (32) can be applicable in this case i.e. the size of the data window length can be reduced to T_0 and as a result, the delay of estimation process can be decreased from $2T_0$ to T_0. The sampling frequency in this test is 40kHz.

Fig. 5 shows the estimation results by the enhanced PM for a set of three phase signals having fundamental and odd-order harmonics same as that of (33) but the dc offsets are 0.038 pu, 0.04 pu, 0.43 pu in phases *a*, *b*, and *c* respectively. The comparison between Fig. (4) and (5) reveals that the phasor measurement method enhanced by the manipulation of positive sequence components produces oscillatory errors when different levels of DC offset are dealt with in three different phases. The magnitude of the error varies in a direct relation upon the amount of differences among the offsets. However, the error is less compared to that of Fig. 1(*b*). The basic PM method of (18) that is set to work with the same data widow size of the enhanced technique, i.e. T_0, produces larger errors like those in Fig. 1(*b*) even dealing with equal offsets in the three phases.

The basic PM method of (18) with the data widow size of T_0 is also predicted to fail on frequency estimation when even-order harmonics appear in the signal. Fig. 6 shows the frequency estimation result for this method when 0.05 pu of the second order harmonic is added to the signal of (34). The test signal in this case can be expressed as

$$\hat{Y}(t) = Y(t) + 0.05e^{j(2\omega t)} \tag{35}$$

where $Y(t)$ is the signal defined in (34).

However, the basic PM based on (27) can give a precise estimation result for the signal of (35) which looks much like

that in Fig. 1(*a*), albeit at the expense of 2 T_0 delay in tracking the online frequency.

4.2. Frequency tracking while amplitude changing

The signal of (33) encounters a sudden amplitude change in the fundamental component from 1 *pu* to 1.4 *pu* at t = 500ms. Fig. 7 shows the result of frequency estimation in this case that the basic PM based on (27) has been utilized. The enhanced PM also produces the same result if the signal of (34), that is free of even order harmonics, is being applied instead of (33). The PM technique is robust against the amplitude changes and does not lose the track of the frequency when sudden changes occur in the signal amplitude.

4.3. Frequency tracking while phase angle changing

The fundamental component of the signal of (33) is subject to a sudden drop of 10^o in its phase angle at $t = 500ms$. Fig. 8 shows the result of frequency estimation by the basic PM technique based on (27) that was proven in the previous section to yield precise estimates. The estimates in this case still remain accurate unless the PM-dada window involves the sample of the angle drop instant. The obtained results during the time frame of $2T_0$ or $40ms$ are subject to significant error as it takes this amount of time for the data window to pass over the angle drop point. The enhanced PM also suffers from the same error but it lasts for $20ms$ in this case. It can be concluded that the phasor measurement technique is not a good choice for frequency estimation when phase angle shifts are likely to happen in the input signal. In other words, vital control or protection decisions should not be made based on the frequency estimation results provided by a PM method at least within its transient response time of $2T_0$ unless it is enhanced by other faster methods like those based on advanced zero-crossing detection [1-3].

4.4. Tracking of frequency changes as a result of applying droop control

Fig. 9 shows a micro-grid in which two DG sources share a variable load. The DGs are assumed to be ideal DC voltage sources supplying DC voltages to their converters. Each converter contains three H-bridges. The outputs of each H-bridge are followed by single-phase transformers connected in Y. The H-bridges and transformers constitute the part of circuit shown schematically in Fig. 9 as VSC. The filter capacitor and the output inductance of the converters are denoted by C and L_f. The resistance R_1 and inductance L_1 represent the impedance of a transmission line between DG_1 and the load. The VSC is controlled through a closed-loop feedback system based on the LQR method [23]. The frequency and voltage droop strategy are applied to both of the DGs in the system. The output voltages and frequency of the converters are controlled to share the load proportional to the rating of the DGs. Let the mean of real and reactive powers supplied by DG_1 in one cycle be denoted by p and q, respectively. The power requirement can be fulfilled by drooping the voltage magnitude and frequency as [23]

$$f = f_0 - m\left(p_{rated} - p\right) \tag{36}$$

$$V = V_{rated} - n\left(q_{rated} - q\right) \tag{37}$$

The variable load is changing randomly from 0.5 *pu* to 1.5 *pu* until t=0.3*s* due to random switching on/off of customer

load. Therefore, (36) implies that the system frequency will vary. After t=0.*3s* the load is maintained constant that leads to a constant system frequency. Fig. 10 shows the reference frequency in a solid graph that the droop control method forces the main control system to follow. Also, the frequency result computed by the enhanced PM technique on the 40 kHz based samples of output voltages of the converter is shown by a dotted graph in Fig. 10. The delay and error between the reference frequency and the computed frequency relate to three factors. First, p and q are obtained from a low pass filter or by averaging in a period. This does not exactly determine the variations of real and reactive power in accordance with the customer demand and also includes a delay due to filtering or averaging. Second, the threshold used in the switching control law and the switching frequency have limitations that lead to error for the state feedback control in tracking the reference state [23]. Third, the advanced PM technique has its own delay of 20 *ms* as per (32). However, the response of the proposed method in this application area is also good.

5. Practical test

A laboratory prototype of a seven-level H-bridge inverter [24], shown in Fig. 11, has been implemented to practically verify the proposed method. The laboratory prototype has been arranged with the same specification defined in [24] and in particular the reference frequency is attempted to be maintained at157.5Hz. Therefore, the key specifications are as follow: V_{dc}=90 V, $I_{out\text{-}peak}$=5 A, f_{sw}=6 kHz and the load is pure inductive with L=16mH. A predictive current control has been developed in a V850E/IG3 microcontroller to force the load current to follow the reference. The output voltage is shown in Fig.12.a. It can be concluded that the signal is highly distorted by harmonics, offset and noise. The basic PM technique has been applied on the samples of the signal at 40kHz. The result of frequency estimation for the signal in Fig. 12,a has been shown in Fig.12.b by a solid line graph. Besides, the reference frequency has also been shown by a dashed line graph in the same figure. The reference frequency is obtained by applying the same PM method on the signal after it is passed through a low pass digital filter. The digital filter has been designed with a data window length equal to the fundamental period of the signal to extract the fundamental component properly. This causes a delay of half cycle time on the frequency estimates. However, the frequency estimation graph relevant to the filtered signal has been shifted to right to be viewed synchronized with the main graph, the solid line one. Fig. 12 reveals that the PM method can successfully track the variations of the signal frequency, despite the high level of distortion in the signal.

6. Conclusion

Analysis of the phasor measurement method for tracking the fundamental power frequency has been presented. The analysis shows that this method performs extremely well especially in presenting precise results for signals highly polluted by harmonics, noise and offset components. However, it suffers from a long delay equal to 40*ms*. A new method has been proposed to lower the delay for special types of signal that are free from even-order harmonics. The PM technique was found to be highly robust against the amplitude changes but unreliable at the transient response against phase angle shifts.

6. Acknowledgment

The authors thank the Australian Research Council (ARC) for the financial support for this project through the ARC Discovery Grant DP 0774092.

7. References

[1] M. M. Begovic, P. M. Djuric, S. Dunlap, A. G. Phadke, "Frequency tracking in power networks in the presence of harmonics," IEEE Transactions on Power Delivery, Vol. 8, pp. 480-486, April 1993.

[2] R. Aghazadeh, H. Lesani, M. Sanaye-Pasand, B. Ganji, "New technique for frequency and amplitude estimation of power system signals," IEE Proceedings on Generation, Transmission and Distribution, vol. 152, pp. 435-440, May 2005.

[3] M. Sanaye-pasand, R. Aghazadeh, "A new technique for frequency estimation of distorted power system signals," International Power System Protection Conference (PSP2002), Slovenia, September 2002.

[4] P. J. Moore, R. D. Carranza, A. T. Johns, "A new numeric technique for high-speed evaluation of power system frequency," IEE Proceedings on Generation, Transmission and Distribution, vol. 141, pp. 529-536, Sept. 1994.

[5] M. M. Begovic, P. M. Djuric, S. Dunlap, A. G. Phadke, "Frequency Tracking In Power Networks Of Harmonics," ICHPS V International Conference on Harmonics in Power Systems., September 22-25, 1992 Page(s):151 – 157

[6] D. W. P. Thomas and M. S. Woolfson, "Voltage and current phasor estimation during abnormal conditions for transmission line protection schemes," in IEE Sixth Int. Conference on Developments in Power System Protection, Univ. of Nottingham, UK, Mar. 25–27, 1997, pp. 266–269.

[7] ---, "Evaluation of a novel frequency tracking method," IEEE Transmission and Distribution Conference, New Orleans, Apr. 11–17, 1999.

[8] P. J. Moore, J. H. Allmeling, and A. T. Johns, "Frequency relaying based on instantaneous frequency measurement," IEEE Trans. on Power Delivery, vol. 11, pp. 1737–1742, Oct. 1996.

[9] A. A. Girgis and W. L. Peterson, "Adaptive estimation of power system frequency deviation and its rate of change for calculating sudden power system overloads," IEEE Trans. on Power Delivery, vol. 5, pp. 585–594, Apr. 1990.

[10] A. G. Phadke, J. S. Thorp, M. G. Adamiak, "A new measurement technique for tracking voltage phasors, local system frequency, and rate of change of frequency," IEEE Transactions on Power Apparatus and Systems vol. 102, pp. 1025-1038, May 1983.

[11] J. Yang and C. Liu, "A precise calculation of power system frequency," IEEE Transaction on Power Delivery, vol. 16, pp. 361-366, July 1993.

[12] D. W. P. Thomas,M. S. Woolfson, "Evaluation of frequency tracking methods,", IEEE Transaction on Power Delivery, vol. 16, pp. 367-371, July 2001.

[13] P. K. Dash, A. K. Pradhan, G. Panda, "Frequency estimation of distorted power system signals using extended complex Kalman filter," IEEE Transaction on Power Delivery, vol. 14, pp. 761-766, July 1999.

[14] A. Routray, A. K. Pradhan, K. P. Rao, "A novel Kalman filter for frequency estimation of distorted signals in power systems," IEEE Transactions on Instrumentation and Measurement, vol. 51, pp. 469-479, June 2002.

[15] A. A. Girgis, T. L. D. Hwang, "Optimal estimation of voltage phasors and frequency deviation using linear and non-linear Kalman filtering: theory and limitations," IEEE Transactions on Power Apparatus and Systems, vol. PAS-103, pp. 2946-2951, Oct. 1984.

[16] M. S. Sachdev, M. M. Giray, "A new numeric technique for high-speed evaluation of power system frequency," IEEE Transactions on Power Apparatus and Systems, vol. PAS-104, pp. 437-444, Feb. 1985.

[17] M. M. Giray, M. S. Sachdev, "Off-nominal frequency measurements in electric power systems," IEEE Transactions on Power Delivery, vol. 4, pp. 1573-1578, July 1989.

[18] V. V. Terzija, M. B. Djuric, B. D. Kovacevic, "Voltage phasor and local system frequency estimation using Newton type algorithm," IEEE Transactions on Power Delivery, vol. 9, pp. 1368-1374, July 1994.

[19] P.K. Dash, B. R. Mishra,R. K. Jena, A. C. Liew, "Estimation of power system frequency using adaptive notch filters," International Conference on Energy Management and Power Delivery, 1998. Proceedings of EMPD '98. 1998, vol. 1, pp. 143-148, March 1998.

[20] H. Karimi, M. Karimi-Ghartemani, M. R. Iravani, "Estimation of frequency and its rate of change for applications in power systems," IEEE Transactions on Power Delivery, vol. 19, pp. 472-480, April 2004.

[21] S. –K Chung, "Phase-locked loop for grid-connected three-phase power conversion systems," IEE Proceedings on Electric Power Applications, vol. 147, pp. 213-219, May 2000.

[22] M. C. Chandorkar, D. M. Divan, Y. Hu, B. Banerjee, "Novel architectures and control for distributed UPS systems," Applied Power Electronics Conference and Exposition, 1994. APEC '94. Conference Proceedings 1994, Ninth Annual 13-17 Feb. 1994 Page(s):683 - 689 vol.2.

[23] A, Ghosh, G. Ledwich, "Power quality enhancement using custom power devices," (Boston, Kluwer Academic Publisher, 2002)

[24] A. Nami, F. Zare, A. Ghosh, F. Blaabjerg, "Hybrid cascade converter topology with series connected symmetrical and asymmetrical diode-clamped H-bridge cells", IEEE Transaction on Power Electronics, web-published on August 19, 2009.

Figures

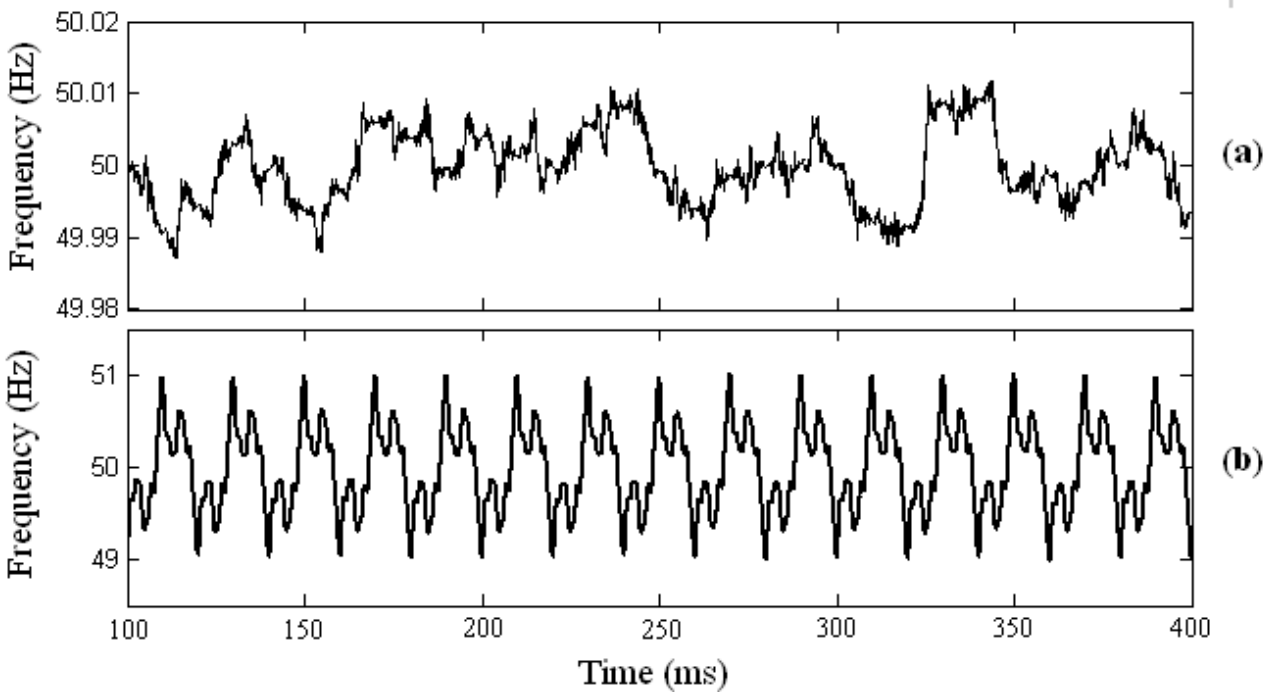

Fig. 1. Frequency estimation by PM technique with the data window size of $2T_0$ (a) and T_0 (b)

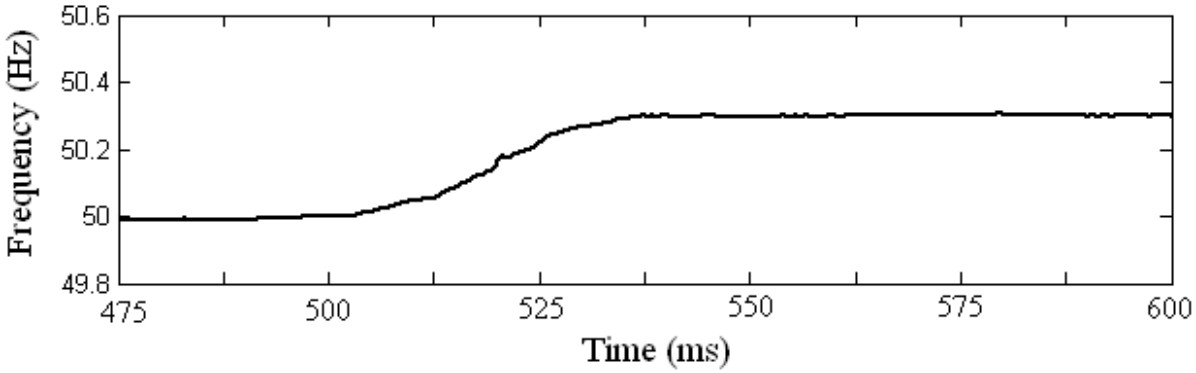

Fig. 2. Response of PM technique to the sudden frequency rise of 0.3Hz

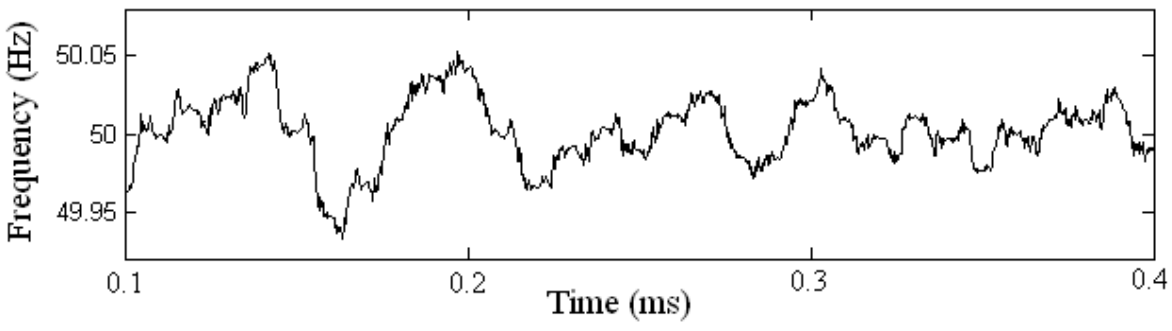

Fig. 3 Frequency estimation by PM technique based on 5kHz sampling rate

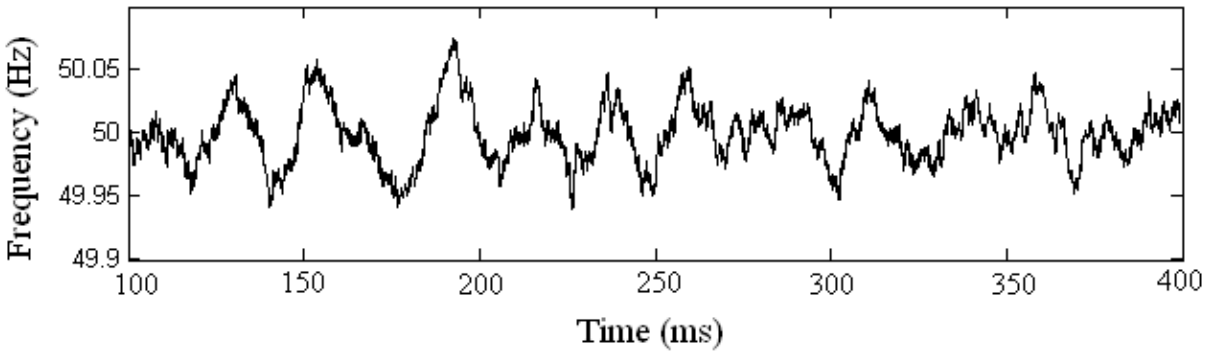

Fig.4. Frequency estimation by PM technique using positive sequence components while data window size of T_0

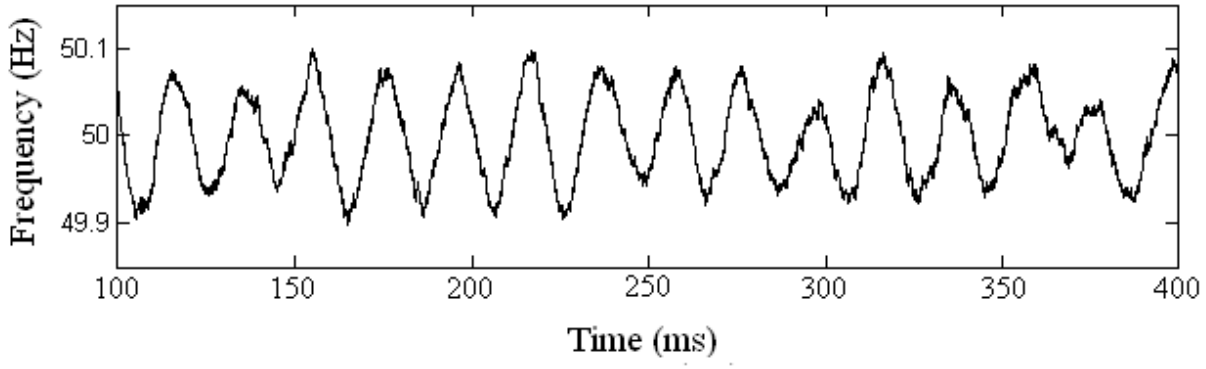

Fig.5. Frequency estimation of a three-phase signal of different offsets in phases using the PM technique enhanced through positive sequence components

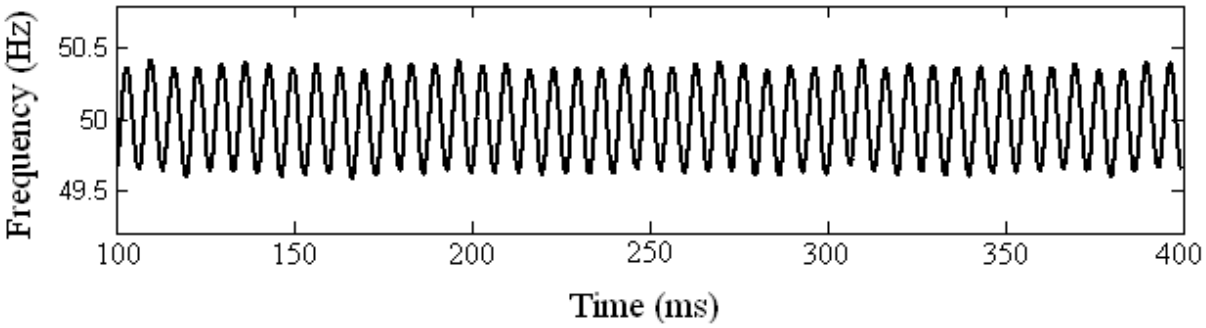

Fig.6. Frequency estimation using the PM technique enhanced through positive sequence components while even harmonics are present in the signal

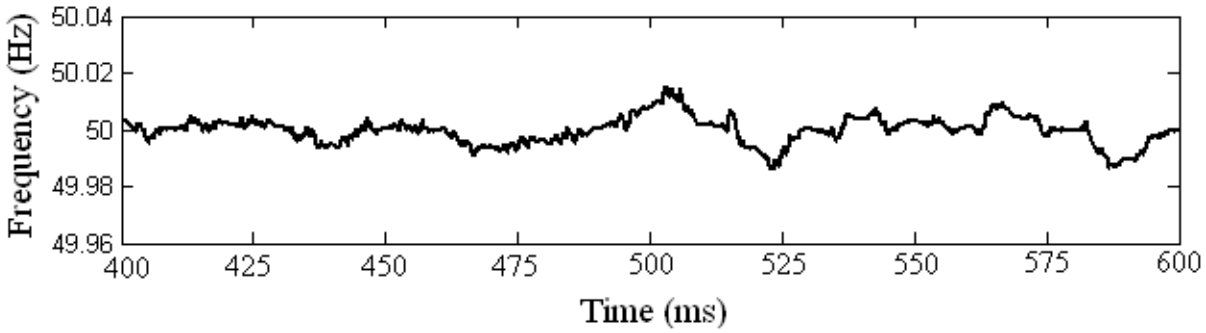

Fig. 7. Frequency estimation by PM technique while the signal amplitude rises suddenly in the fundamental component for 0.4 pu

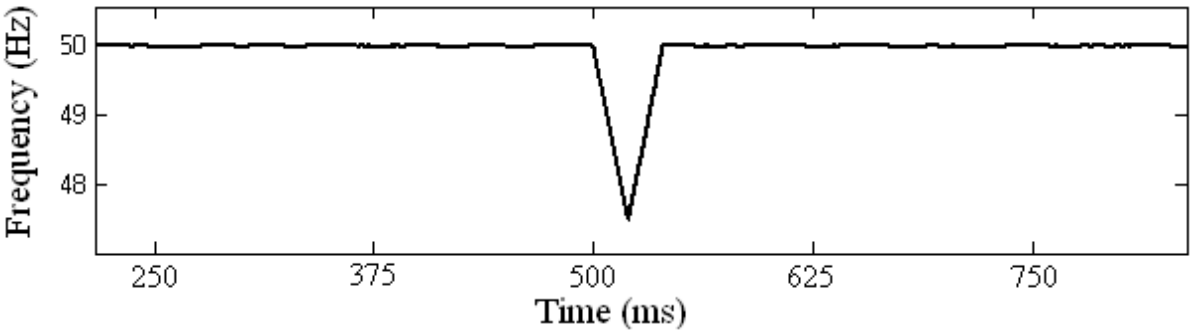

Fig. 8. Frequency estimation by PM technique while the phase angle of the fundamental component drops suddenly for 10o

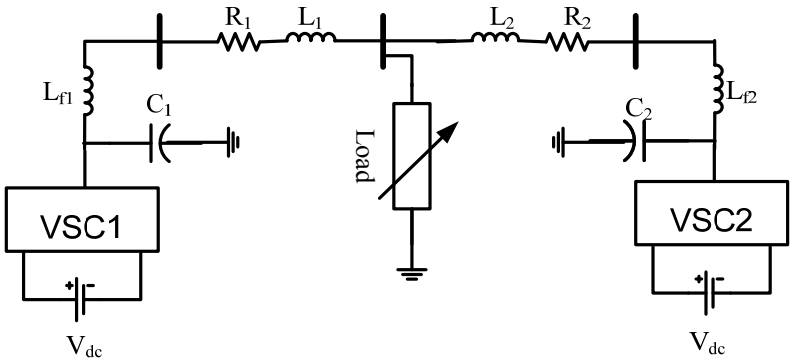

Fig. 9. Schematic diagram of two DG sources connected to a micro-grid

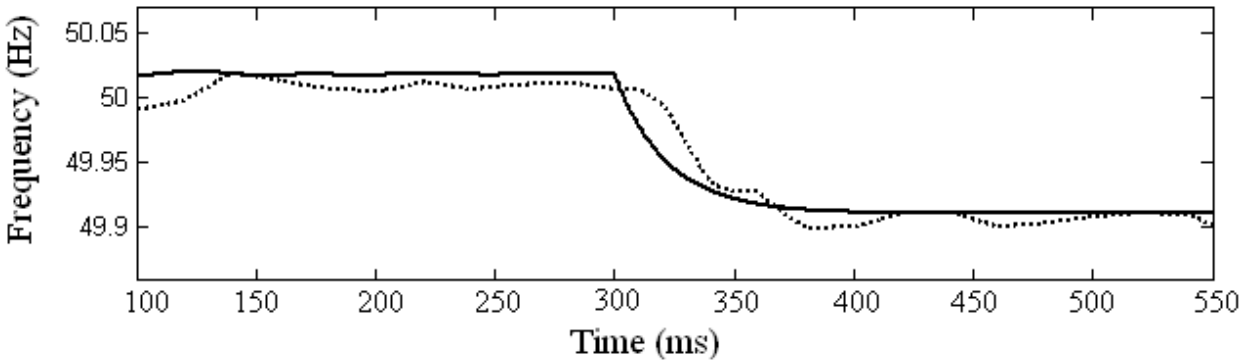

Fig. 10. Frequency estimation by PM technique in a micro-grid system; solid line: the reference frequency and dotted line: the estimated frequency

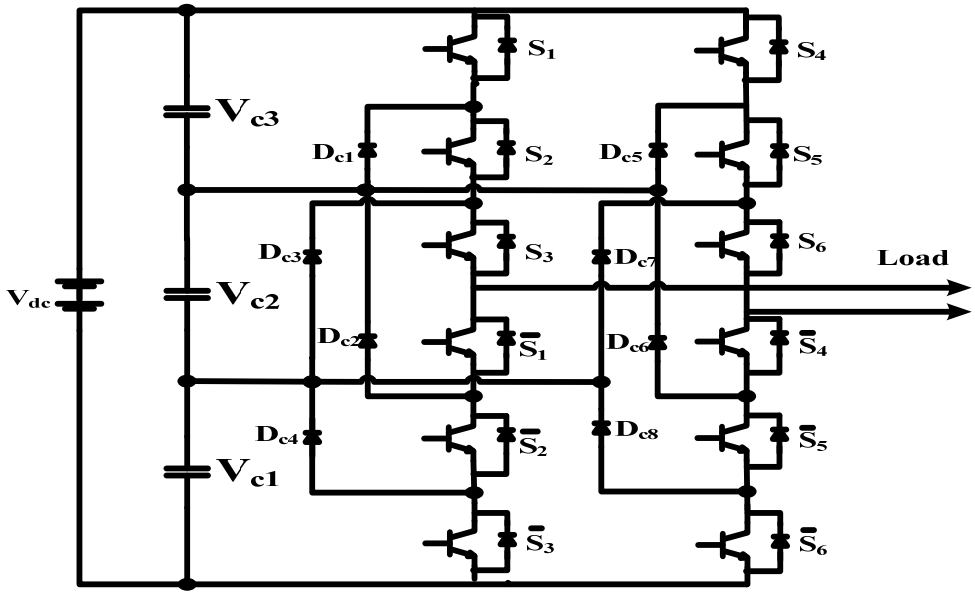

Fig. 11. A laboratory prototype of a seven-level H-bridge inverter [24]

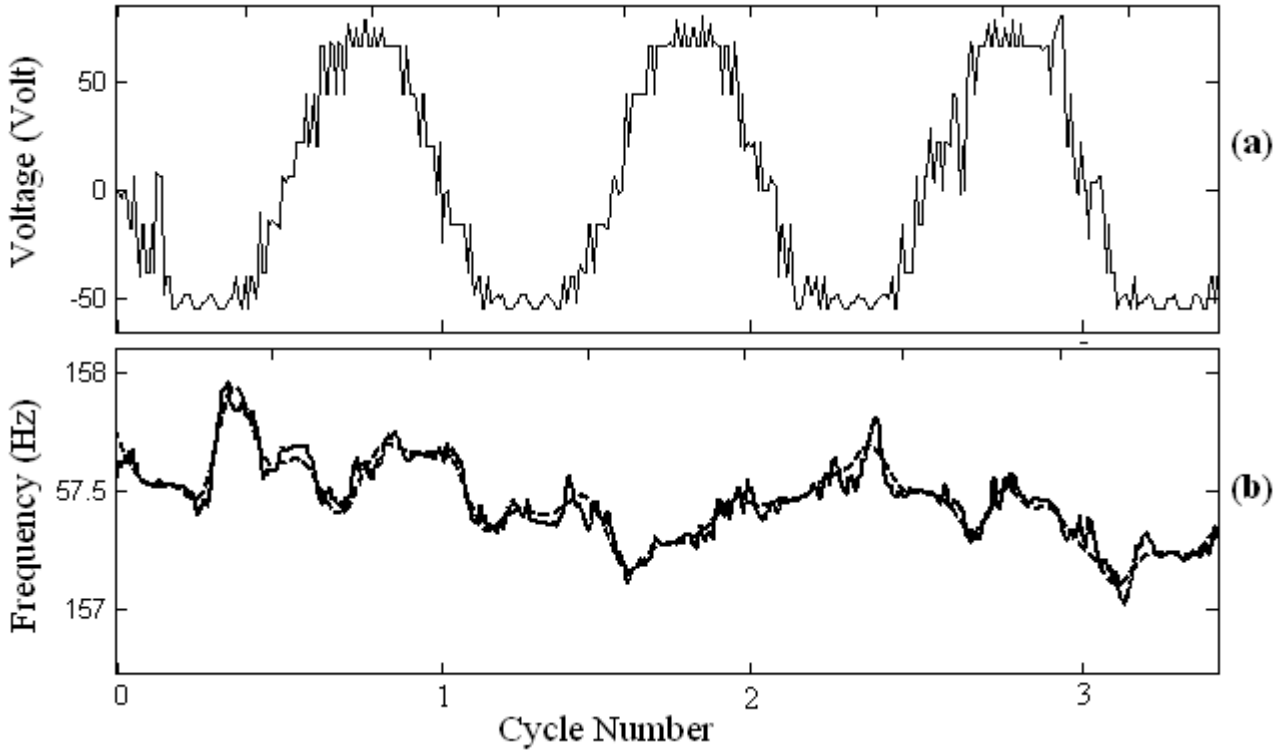

Fig. 12. Output voltage of the H-bridge inverter (a), and its frequency estimation result by the basic PM shown in solid-line graph in conjunction with the reference frequency computed for the extracted fundamental component shown in dashed-style graph (b)